Manchester Metropolitan University

e-space

Manchester Metropolitan University's Research Repository

Please cite the Published Version

Vadivel, Srinivasan, Sengodan, Boopathi C, Ramasamy, Sridhar, Ahsan, Mominul, Haider, Julfikar and Rodrigues, Eduardo MG (2022) Social Grouping Algorithm Aided Maximum Power Point Tracking Scheme for Partial Shaded Photovoltaic Array. Energies, 15 (6). p. 2105.

DOI: https://doi.org/10.3390/en15062105

Publisher: MDPI AG

Version: Published Version

Downloaded from: https://e-space.mmu.ac.uk/629343/

Usage rights: CC BY Creative Commons: Attribution 4.0

Additional Information: This is an Open Access article published in Energies.

Enquiries:
If you have questions about this document, contact openresearch@mmu.ac.uk. Please include the URL of the record in e-space. If you believe that your, or a third party's rights have been compromised through this document please see our Take Down policy (available from https://www.mmu.ac.uk/library/using-the-library/policies-and-guidelines)

energies

MDPI

Article

Social Grouping Algorithm Aided Maximum Power Point Tracking Scheme for Partial Shaded Photovoltaic Array

Srinivasan Vadivel [1], Boopathi C. Sengodan [1], Sridhar Ramasamy [1,*], Mominul Ahsan [2], Julfikar Haider [3] and Eduardo M. G. Rodrigues [4,5,*]

1 Department of Electrical and Electronics Engineering, SRM Institute of Science and Technology, Chennai 603 203, India; sv6465@srmist.edu.in (S.V.); boopathc1@srmist.edu.in (B.C.S.)
2 Department of Computer Science, University of York, Deramore Lane, York YO10 5GH, UK; md.ahsan2@mail.dcu.ie
3 Department of Engineering, Manchester Metropolitan University, John Dalton Building, Chester Street, Manchester M1 5GD, UK; j.haider@mmu.ac.uk
4 INESC-ID, Sustainable Power Systems Group, Av. Rovisco Pais 1, 1049-001 Lisboa, Portugal
5 Instituto Superior Técnico, University of Lisbon, Av. Rovisco Pais 1, 1049-001 Lisboa, Portugal
* Correspondence: sridharr@srmist.edu.in (S.R.); eduardo.g.rodrigues@tecnico.ulisboa.pt (E.M.G.R.)

Abstract: Photovoltaic (PV) systems-based energy generation is relatively easy to install, even at a large scale, because it is scalable in size and is thus easy to transport. Harnessing maximum power is only possible if maximum power tracking (MPPT) functionality is available as part of the power converter control that interfaces the PV panels to the grid. Solar exposure covering all PV panels is unlikely to happen all the time, which is known as a partial shading (PS) phenomenon. As a result, depending on the MPPT algorithm adopted, it may fail to find a maximum global power peak, being locked into a local power peak. This research work discusses an alternative MPPT control technique inspired in the social group optimization (SGO) algorithm. SGO belongs to the meta-heuristic optimization techniques family. In this sense, the SGO method ability for solving global optimization problems is explored to find the global maximum power point (GMPP) under the presence of local MPPs. The introduced SGO–MPPT was subjected to different PS conditions and complex shading patterns. Then, its performance was compared to other global search MPPT techniques, which include particle swarm optimization (PSO), the dragon fly algorithm (DFO) and the artificial bee colony algorithm (ABC). The simulation outcomes for the SGO–MPPT characterization showed good results, namely rapid global power tracking in less than 0.2 s with reduced oscillation; the efficiency of solar energy harness was slightly above 99%.

Keywords: photovoltaic; partial shading; maximum power point tracking; social group algorithm; soft computing; DC-DC converter

check for updates

Citation: Vadivel, S.; Sengodan, B.C.; Ramasamy, S.; Ahsan, M.; Haider, J.; Rodrigues, E.M.G. Social Grouping Algorithm Aided Maximum Power Point Tracking Scheme for Partial Shaded Photovoltaic Array. *Energies* **2022**, *15*, 2105. https://doi.org/10.3390/en15062105

Academic Editors: Luigi Costanzo and Gregorio García

Received: 15 December 2021
Accepted: 8 March 2022
Published: 13 March 2022

Publisher's Note: MDPI stays neutral with regard to jurisdictional claims in published maps and institutional affiliations.

Copyright: © 2022 by the authors. Licensee MDPI, Basel, Switzerland. This article is an open access article distributed under the terms and conditions of the Creative Commons Attribution (CC BY) license (https://creativecommons.org/licenses/by/4.0/).

1. Introduction

The rate of deployment of new PV power plants has not decelerated over the last few years. The most recent figures for the year 2020 show a world-wide growth rate of 22%. Presently, the installed PV power in the electricity grid is ranked third, below hydroelectric and wind power generation [1,2]. As in the Western societies that are taking the first steps for a non-carbon economy, developing countries are making efforts in this direction as well. India, for example, with its huge population and vast solar resources, has an ambitious clean energy target of 175 GW, which is to be deployed by 2022 [3]. Therefore, PV technology will play a significant role in a future carbon-free society since wind power resources, despite their abundant availability, is limited by its natural intermittence and requires suitable areas for the erection of wind farms. COVID-19 has indirectly impacted the growth of the PV industry also, as supply chain disruption, closure of sites, and power purchase agreements have taken a back seat [4]. Despite several hurdles, the investment in

PV and research interest in PV power enhancement will not fade away, as PV possesses unique advantages of being clean and green, scalable and portable. The power output of PV cannot be constant and continuous due to the variations in temperature and irradiation. However, the usage of a power converter as an interface between the PV and the load is indispensable. The power converter facilitates the following two important functions:

1. Voltage regulations and enhanced compatibility between the PV and load;
2. Ensuring maximum power point tracking (MPPT).

MPPT is a controller that is integrated with a converter which operates the PV panel to yield maximum available power in the PV at any given point in time. MPPT relies on a control algorithm that caters to the operating peak voltage (V_{mp}) at which the PV power is maximum in the nonlinear power–voltage (P–V) curves [5]. The most prominent MPPT algorithm is P&O, which is reliable and easy to execute. Here, a small perturbation is introduced in the P–V curves and the search travels along the curve to find the peak of the curve for the given irradiation and temperature [6]. If the power yield through the search is not progressive, then a change in the direction of search is introduced. Conversely, the major drawback of P&O is that even after grasping the peak, it tends to hover around the peak power, which makes the system sluggish. The other reliable technique which discards the oscillation is the incremental conductance (INC), where the peak power is tracked through the maximum slope method. Here, through appropriate sensors and processes, the ratio between incremental conductance and instantaneous conductance of the PV module is equated. This technique is prone to error when irradiation changes dynamically. Therefore, improved versions of both the P&O and INC have attracted much attention among researchers. There are also few simpler power tracking schemes such as open circuit voltage (OCV) and short circuit current (SCC) [7,8]. Among these, the OCV method is preferable for lower power-rated applications and where there is minimal temperature variations. However, these conventional algorithms face a huge setback when they are bound to search the power curves, having multiple power peaks due to partial shading. Partial shading (PS) is a phenomenon in which the PV panels in a PV array receives irradiation in an inhomogeneous way, i.e., few panels receive full irradiation, whereas the remaining panels receive irradiation only partially. The PV curves of the shaded array exhibit multiple power peaks, and the conventional MPPTs above stick to the local maximum. Most of the time, they will not grasp the global power peak, which in turn results in significant losses and hot spot formation on the panels [9,10].

To overcome this pertinent issue, bio-inspired and artificial intelligence (AI)-aided MPPT schemes are proposed in the PV research arena. These intelligent algorithms have the rationale to evade the local power peak and grasp the global one. Genetic algorithm (GA) [11] and particle swarm optimization algorithms (PSO) were the first ones to address the failure MPPT during shading [12–15]. These algorithms initialize its searching parameters over the search space randomly, and during the search, there exists a communication between the particles and a sharing of the cognizance acquired through the travel [16]. In the PSO MPPT, the randomly initiated particles over the searching space obtain their updated position and then share that knowledge on position among themselves. After each iteration, finally, all particles reach the global power peak [17]. The randomness of PSO particle initialization with unwanted oscillations gives scope for further deep research in PSO MPPT, where a modified version of the PSO such as improved PSO and hybrid PSO MPPT are introduced. The gravitational search inclusion along with the PSO makes a new algorithm termed as hybrid particle swarm optimization gravitation search (PSOGS), which is effective in convergence with a smaller number of iterations. However, the PSOGS increases the number of parameters involved and results in coding complexity. Among the evolutionary algorithms, artificial neural network (ANN) [18] rendered its contribution to the MPPT in many aspects. The datasets needed for training will either voltage–current or irradiation–temperature. Differential evolution (DE) MPPT was preferred since it has minimum parameters, but a major drawback is its inability to specify the searching direction of the candidates involved. Tey et al. [19] proposed a modified DE MPPT where the search

direction is given during the mutation phase. However, overall, the DEMPPT is not often used for MPPT owing to its sluggish nature and random search, which causes high variance in the output power. Ant colony algorithm (ACO) [20], conversely, has attracted much attention among PV researchers, who intended to effectively charge the batteries through partially shaded PV panels. Another interesting work on global MPPT was proposed by Benyoucef et al. [21], where the authors used a two-stage control scheme, blending the conventional P&O scheme and inventive artificial bee colony (ABC) algorithm. However, the ABC did not render a complete solution, as the convergence was not effective for connecting more strings of the PV panels. Again, the grey wolf optimizer (GWO) [22], known for its higher efficiency, needs more population. Numerous bio-inspired algorithms have been archived in the research arena, which defends its own competency on convergence and efficacy. Still, the quest for proposing a new algorithm for MPPT in a partially shaded PV array continues with the same vigour. In addition, to prevail over the rapidly varying irradiation pattern and to grasp the global peak, more communal thinking is needed. The research arena has recently witnessed a group teaching algorithm [23–26] in which teachers teach the students to make them knowledgeable. The knowledge-acquiring capability will vary from one student to another, and the peer group also helps to enhance the knowledge. However, it needs more people to form the group effectively, and the time taken for improving the worst person with respect to converging towards the best will increase.

The stochastic social grouping algorithm (SGO) has competencies such as fast convergence and less oscillation. These traits are essential for a nonlinear objective function such as maximum power point tracking. SGO is a new algorithm which has not been tested for the MPPT application. Here in this work, SGO is used to have its fullest merits, as it possesses unique features such as minimal control parameters (only one), and during each iteration, the best candidate is identified twice. Satapathy and Naik [27] have provided insights about the implementation of the SGO with respect to acquiring knowledge and improving knowledge phases for civil infrastructure applications. Although the SGO is a competent global search algorithm, its fullest efficacy has not been utilized yet in the research forum. Given the traits of the SGO, it is a suitable candidate for a global power search in the shaded PV array. This research proposal intends to deploy SGO–MPPT for an 800 W PV system. In this work, the versatility of the SGO–MPPT is tested for different shading patterns, and its performance is compared with other bio-inspired counterparts. This paper is organized in such a way that the details of PV, shading impact and boost converter design are discussed in Section 2, while the details about the social group optimization are presented in Section 3. The SGO–MPPT and its competency is detailed in Section 4 through various case studies. Finally, Section 5 presents conclusive remarks.

2. PV Cell Modelling and Partial Shading Impact

The knowledge of the mathematical model of PV and the impact of shading on PV output is fundamental to further analysis. In this section, the PV model and the impact of partial shading are discussed.

2.1. PV Modelling

An ideal PV cell is represented by a current source in parallel to a PN junction, with its anode connected to the positive terminal of the current source [28]. A practical PV cell will be in series and have shunt resistance as shown in

The photoelectric effect is modelled with a current source I_{ph}. The leakage current takes two paths: one through a PN junction called I_d and the other through a parallel resistor R_{sh} designated as I_{sh}. The series resistor R_s takes into account cell internal power dissipation. The output current I_{PV} is expressed as:

$$I_{PV} = I_{ph} - I_D - I_{sh} \quad (1)$$

Replacing I_D with the diode expression and I_{sh} with $\frac{V_D}{R_{sh}}$, Equation (1) is updated as [29]:

$$I_{PV} = I_{ph} - I_O \left\{ \exp\left[\frac{(V_{PV} + I_{PV} \times R_s)}{\left(\frac{\eta k_b T}{q}\right)} \right] - 1 \right\} - \frac{V_{PV} + I_{PV} \times R_s}{R_{sh}} \quad (2)$$

where I_O refers to the diode reverse saturation current, q is the electron charge (1.602×10^{-19} C), k_b is the Boltzmann constant ($1.3806503 \times 10^{-23}$ J/K), T takes into account cell temperature in *kelvin*, and η is the ideality factor. Any practical evaluation in a simulation scenario requires a more complete circuit to reproduce a solar panel I–V curve, normally made up of parallel strings of cells. In Figure 2, N_s and N_p refer to the number of cells connected in series and parallel. respectively. In this work, four PV panels (PV1, PV2, PV3 and PV4) of 200 W are connected in series to form a PV array of 800 W. Figure 1.

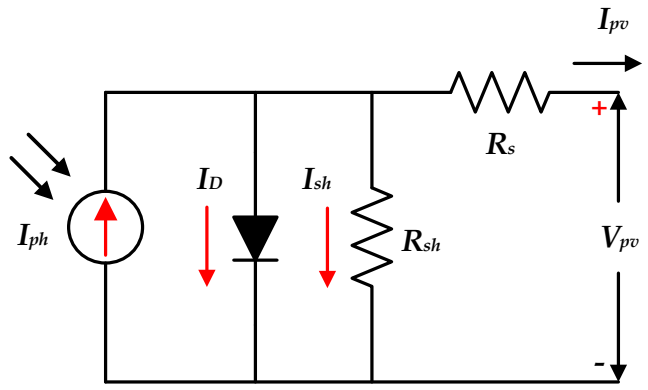

Figure 1. Electrical equivalent diagram for single diode PV model.

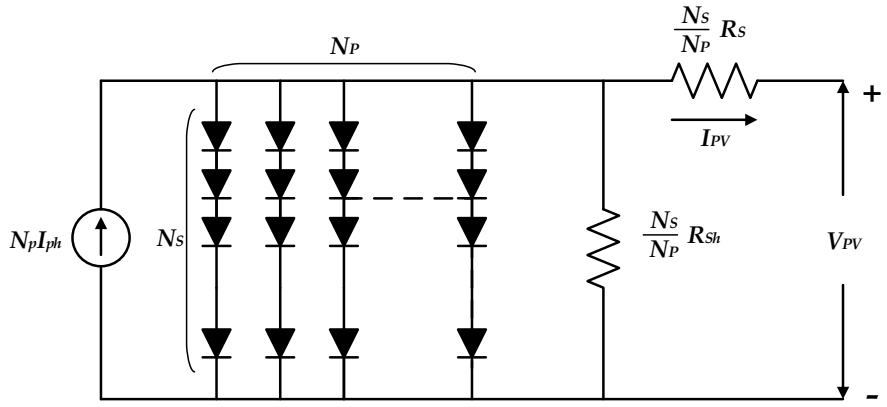

Figure 2. PV cell panel equivalent circuit.

Then, the panel behaviour can be approximated as:

$$I_{PV} = N_p I_{ph} - N_p I_O \left\{ exp\left[\frac{\left(V_{PV} + I_{PV} \times R_s \frac{N_s}{N_p}\right)}{N_s * \left(\frac{\eta k_b T}{q}\right)} \right] - 1 \right\} - \frac{V_{PV} + I_{PV} \times R_s \frac{N_s}{N_p}}{\frac{N_s}{N_p} R_{sh}} \quad (3)$$

2.2. Partial Shading Effects

Solar panels provide maximum power when the irradiation is uniform over the panels. Partial shading is a phenomenon which occurs due to the proximity of physical objects such as trees, electric power transmission poles or building facades that may project a partial shadow over PV panels. Major impacts of the partial shading are reduced output power, hotspots on the PV panels and panel lifetime degradation [30]. As soon as some of

PV panels that comprise a renewable power plant are partially shaded, the voltage–current (I–V) and power–voltage (P–V) curves will have multiple maxima. Since in these operating conditions the P–V curve has multiple local peaks, the MPPT scheme may have difficulty distinguishing between a local peak and a maximum global power peak, thus causing significant power generation loss. Figure 3a refers to the arrangement of the PV panels without shading presence (left) and with partial shading (right). The corresponding output characteristic curves are depicted in Figure 3b,c.

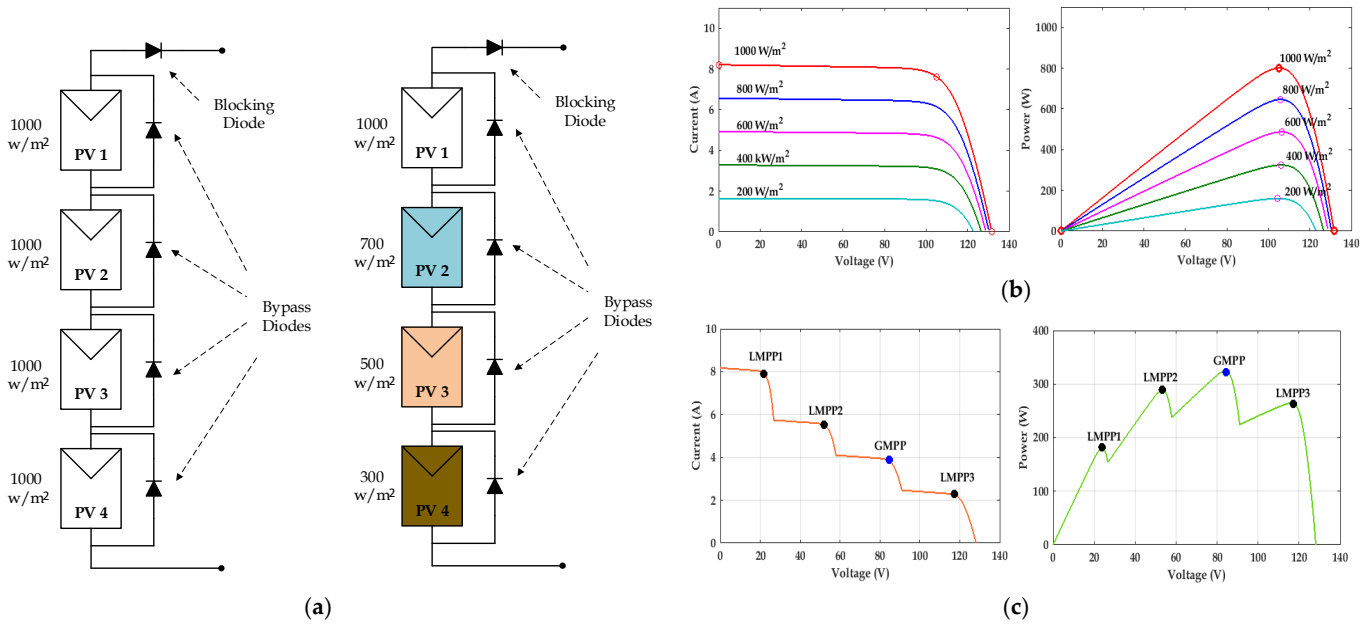

Figure 3. (**a**) Solar array in both scenarios. (**b**) P–V and I–V curves for uniform irradiation and (**c**) P–V and I–V curves for non-uniform irradiation.

The MPPT mechanism ensures the extraction of maximum available power for each combination of solar irradiation and panel temperature. A PV panel rated at nominal power can only supply that value at STC, i.e., the irradiation is 1000 W/m^2, and the cell temperature is 25 °C. From Figure 3b, it is inferred that the peak power of the array changes according to the irradiation level. The operating point that allows maximum power generation is denoted by P_{mp} and the corresponding pair of voltage and current quantities are designated as V_{mp} and I_{mp}, respectively.

2.3. Boost Converter Design

The boost converter provides two functions [31,32]. First, it provides an interface between the PV array and the load. Second, it provides the controlling action for the MPPT controller. The output of the boost converter is adjusted according to the duty cycle of the PWM signal to operate the PV system at GM. The output–input voltages, output–input capacitances, operational frequency, and other electrical parameters are calculated using Equations (4)–(7).

$$\text{Duty Cycle, } D = 1 - \frac{V_{in}}{V_{out}} \tag{4}$$

$$\text{Capacitor, } C_{in} = \frac{i_{IL} D}{8 \Delta V_i f_s} \tag{5}$$

$$\text{Inductor, } L = \frac{V_{in} D}{2 \Delta i_L f_s} \tag{6}$$

$$\text{Capacitor, } C_{out} = \frac{i_o D}{8 \Delta V_o f_s} \tag{7}$$

where V_{in} and V_{out} stand for the input and output voltages, D is the duty cycle calculated by Equation (4), L is the inductance, C_{in} is the input capacitance, C_{out} is the output capacitances, f_s is the switching frequency, ΔV_i is the 1% of input ripple voltage, and Δi_L is the inductor ripple current of the boost converter.

3. SGO-Based MPPT

3.1. SGO Principles

The SGO algorithm [27] emerged from making most of the individual excellence and by leveraging the competencies of individuals in a group. Some individuals possess the capability of solving complex problems and yielding optimized solutions in life. When these individuals are part of a social group, the team members will acquire the cognizance of their fellow mates and emulate the same successful path of problem solving. In SGO, each person is considered to be the candidate solution with traits of having some knowledge of problem solving. This problem-solving capacity is termed as fitness. The best person in the group produces the best solution. The knowledge of problem solving by the best person is transferred as knowledge transfer to other candidates in the group to uplift themselves and in turn results in the group's overall uplift.

The SGO algorithm consists of two phases, where in the first phase, the knowledge of each individual candidate is improved through impact acquired from the best person within the group. In the second phase, each candidate will improve their knowledge through mutual influence from fellow candidates of the group and also from the overall best person within the group. The first phase is called the improving phase, and the second phase is called the acquiring phase. The number of members in the group is termed as N, each individual is termed as X_k, where k represents the number of specific candidates in that group. X_{kD} refers to the dimension of the candidate, which is a reference to the qualities of the individual, and f_k (k = 1, 2, … N) is their associated fitness shown in Figure 4.

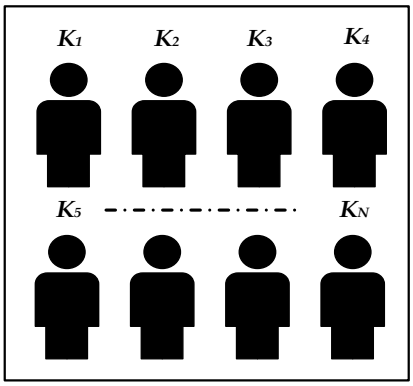

Figure 4. Number of candidates in the group in the SGO algorithm.

3.1.1. Improving Phase

In this phase, each social group's best candidate is called the global best ($gbest_g$) and intends to disseminate the knowledge to other team members. The team members that participate in this learning will enhance their knowledge.

The fitness function for maximization is $gbest_g = max\ \{f_j, j = 1, 2, \ldots, N\}$. In addition, during this phase, for every iteration, the knowledge between the candidates is shared and updated, which can be represented by Equation (8).

$$X_{new\_jk} = C \times X_{old\_jk} + r \times (gbest(k) - X_{oldjk}) \quad (8)$$

where r is random selection, X_{new} is the fitness after each iteration, and X_{new} replaces X_{old} if X_{new} presents better fitness, as shown in Figure 5.

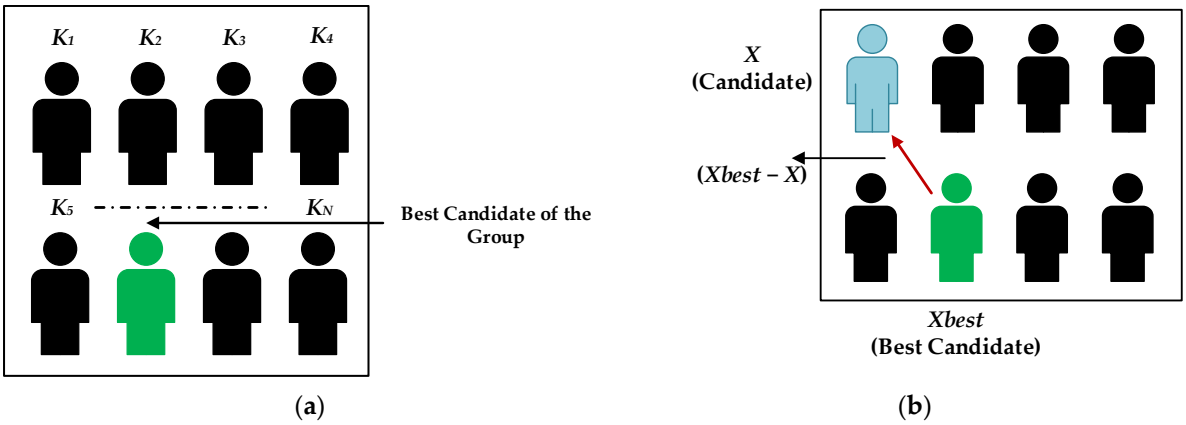

Figure 5. (**a**) Best candidate of the group. (**b**) Best fitness of the candidate in the SGO algorithm.

3.1.2. Acquiring Phase

In this phase, each member of the group obtains knowledge from a highly knowledgeable person and also interacts with other members at random. The candidates will acquire new knowledge from each other as well from the most knowledgeable person ($gbest_g$). If another individual has more knowledge than $gbest_g$, then he will replace the best candidate by himself, as shown in Figure 6.

Randomly selecting one person Xr, where $j = r$

If $f(X_k) > f(X_r)$

$$Xnew_{j,k} = X\,old_{j,k,} + r_1 \times (X_{j,k} - X_{j,k}) + r_2 \times (gbest_k - X_{j,k}) \quad (9)$$

If $f(X_k) < f(X_r)$

$$Xnew_{j,k} = X\,old_{j,k} - r_1 \times (X_{j,k} - X_{j,k}) + r_2 \times (gbest_k - X_{j,k}) \quad (10)$$

Accept X_{new} if it gives a better fitness function value, where r_1 and r_2 are two independent random sequences. As indicated in Equation (10), these sequences are employed to influence the algorithm's stochastic nature.

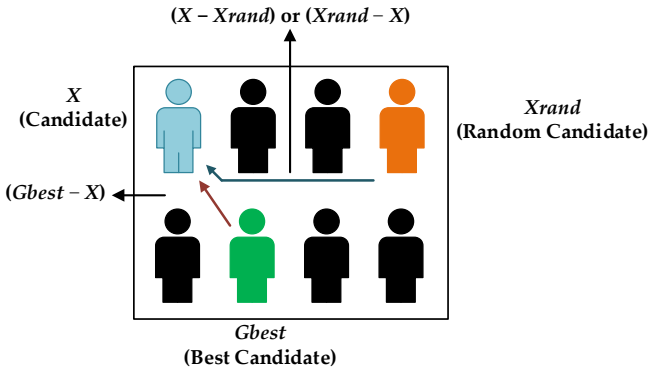

Figure 6. G_{best} candidate of the group in the SGO algorithm.

3.2. SGO–MPPT Implementation

Due to the singular properties of the SGO algorithm, an alternative approach for tracking global maximum power point (GMPP) is discussed for the first time. The execution of SGO–MPPT is shown in Figure 7. The SGO–MPPT arrangement consists of a PV array connected to the load through a boost converter. The control signal for the boost converter is obtained from the SGO algorithm, whose processing runs inside a dedicated controller. The algorithm processes instantaneous voltage and current as inputs to find the optimal duty cycle for GMPP location.

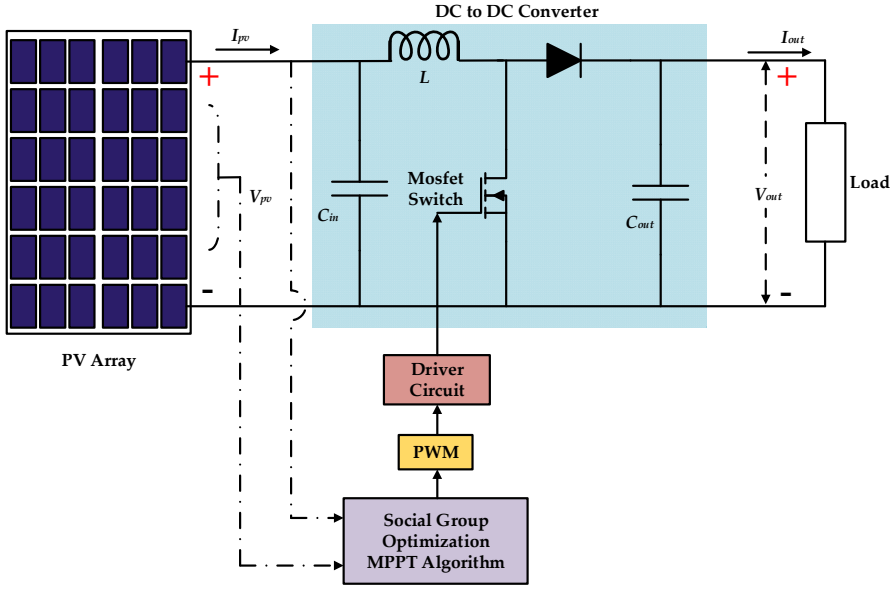

Figure 7. Solar DC–DC converter-integrated SGO–MPPT control.

This section explains how to implement the SGO in a step-by-step manner.

3.2.1. Initialization Phase

Step 1: Generate random population (Candidate/Duty Cycle).

3.2.2. Improving Phase

Step 2: Evaluate Power $D_{new(k)}$ of each candidate and identify G_{best}. Candidate with best power is the best candidate of the group with highest knowledge.

Step 3: In this phase, the knowledge level of each candidate in the group is enhanced by the knowledge of the best candidate (gbest) in the group as defined by Equation (11).

$$D_{newjk} = C \times D_{oldjk} + r \times (G_{best(k)} - D_{oldjk}) \quad (11)$$

where:

D_{newjk}—New Solution of Candidate;
C—Self Introspection (0 to 1);
D_{oldjk}—Existing Solution;
r—Random Number (0 to 1);
$(G_{best(k)} - D_{oldjk})$—Influence of the best Candidate.

A new Solution is accepted if better than existing solution D_{oldjk}. While tracking the global power peak, the values of C and r randomly change.

3.2.3. Acquiring Phase

Step 4: In this phase, every Candidate shall enhance its knowledge by interaction with another random Candidate in the group and the best Candidate in the group.

If $D_{newj,k}$ is better than D_{rand},

$$D_{newj,k} = D_{oldj,k} + r_1 \times (D_{j,k} - D_{randj,k}) + r_2 \times (G_{bestk} - D_{j,k}) \quad (12)$$

If D_{rand} is better than $D_{newj,k}$,

$$D_{newj,k} = D_{oldj,k} - r_1 \times (D_{j,k} - D_{randj,k}) + r_2 \times (G_{bestk} - D_{j,k}) \quad (13)$$

$D_{newj,k}$ is accepted if better than existing solution $Dold_{j,k}$.

Step 5: Update the new G_{best}.

The optimal duty cycle was detected through the sequence of processes where the first stage involved the initialization of four duty cycles (d1, d2, d3, d4). The value of each duty cycle was computed using Equation (11). The respective power instants for these duty cycles were also recorded. The duty cycle at which maximum power occurred was assigned as the global best (G_{best}), and the powers corresponding to the individual duty cycles were considered to be the candidate best (D_{best}). The knowledge sharing of the G_{best} and Drand happened within the candidates through Equations (12) and (13). The updated duty cycle (candidates) was applied to the power converter, which in turn delivered the respective power after each iteration. The search process was sustained for the whole of the subjected iteration value. If the current position of the candidate remained as the best, then the peak power value was unchanged. This procedure of identifying the best duty cycle continued until all the candidates converged to MPP.

To better understand the SGO–MPPT operation, a flow chart is documented in Figure 8. The chart clearly presents how the duty cycle convergence takes place with respect to instantaneous voltage and current during partial shading of the PV panels in a PV array. The flow chart explains the two phases in the SGO–MPPT, namely the improving and acquiring phase.

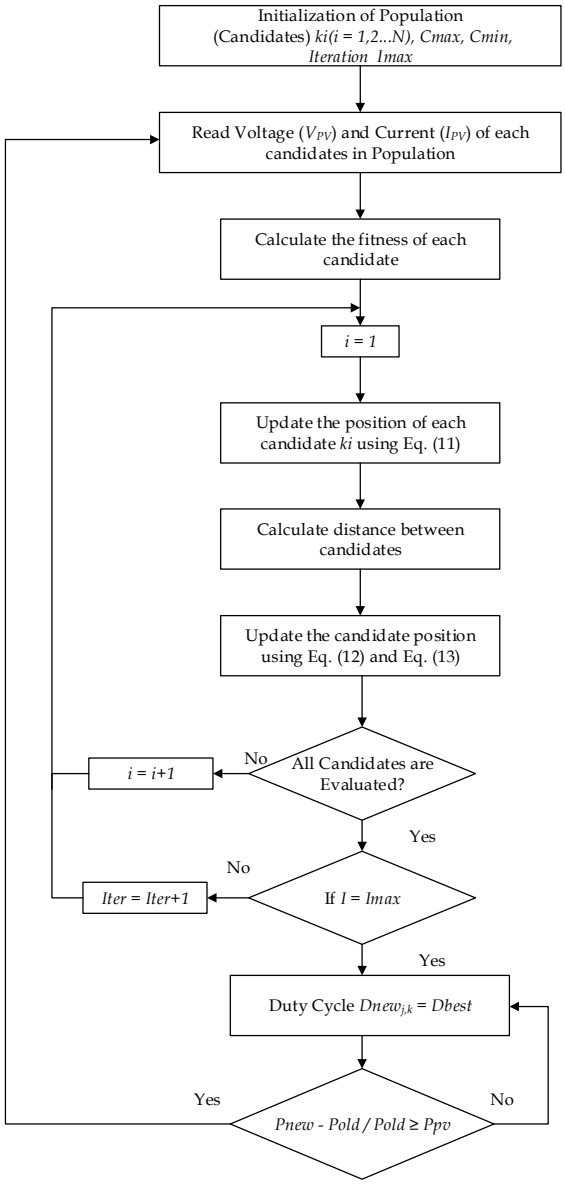

Figure 8. Operational flow chart of the SGO–MPPT process.

4. Results and Discussion

In this section, a detailed analysis of the performance of the SGO–MPPT control is presented.

4.1. Simulation Methodology

Three simulation scenarios with distinct operating conditions were generated in Matlab tool. MPPT strategies based on particle swarm optimization (PSO), particle swarm optimization gravitation search (PSOGS), artificial bee colony algorithm (ABC) and dragon fly algorithm (DFO) optimization algorithms served as the basis for measuring SGO–MPPT effectiveness in finding GMPP.

For accurate modelling of a real PV panel, KC200GT solar panel data from the Kyocera manufacturer were used. Table 1 presents the main specifications of the standard test conditions (STC).

Table 1. Kyocera KC200GT 200 W.

Specifications	Values
Maximum Power (P_{max})	200.143 W
Maximum Power Voltage (V_{mp})	26.3 V
Maximum Power Current (I_{mp})	7.61 A
Open Circuit Voltage (V_{oc})	32.9 V
Short Circuit Current (I_{sc})	8.21 A
Temperature Coefficient of V_{oc}	−0.1230 V/K
Temperature Coefficient of I_{sc}	0.0032 A/K
Number of Cells per Module	54

Simulation parameters of boost converter is C_{in} = 15 µF, L = 369.25 µH, C_{out} = 14.45 µF and R = 13.83 Ω. Table 2 shows the tuning parameters of SGO, DFO, ABC, PSOGS and PSO. An initial population size of four was considered for all MPPT algorithms.

Table 2. Tuning parameters for MPPT algorithms under comparison.

MPPT Method	Tuning Parameters
SGO	C_{min} = 0.1, C_{max} = 0.9
ABC [21]	W_{max} = 0.9, W_{min} = 0.4
PSOGS [33]	C_1 = 0.5, C_2 = 1.5, G_0 = 1, W = 0.9
DFO [34]	S = 0.1, a = 0.1, c = 0.7, f = 1, e = 1
PSO [35]	C_{1max} = C_{2max} = 2, C_{1min} = C_{2min} = 1, W_{max} = 1, W_{min} = 0.1

To test the competency of the SGO algorithm, the shading pattern of the four PV panels in the array was varied dynamically. Three dynamical shading cases were considered as shown in Table 3. Each shading pattern exhibited its own PV peak power. Case 1 provided a fast-changing irradiance profile, whereas Cases 2 and 3 dealt with different partial shading circumstances.

Table 3. PV panels configuration and insolation levels.

Case Study	Solar Irradiance (W/m^2)				P_{max} (W)
	PV 1	PV 2	PV 3	PV 4	
Case 1	1000; 700; 300 *	1000; 700; 300	1000; 700; 300	1000; 700; 300	798; 557.8; 227.3
Case 2	500	800	1000	900	504.2
Case 3	800	300	700	500	322.2

* Changes in radiation after every 2 s.

When there is a change in irradiation, the current increases or decreases linearly, whereas for the temperature change, the voltage changes logarithmically. As a result,

the power variation is minimum [36]. Therefore, it is sufficient to take into account the irradiation alone. Furthermore, the SGO–MPPT suggested here is capable of finding the peak power even if the analysis includes temperature variation, since the output P–V curve embodies the change and the SGO–MPPT is competent enough to grasp the peak power for any nonlinear P–V curves.

4.2. Case Studies

4.2.1. Case 1

In this scenario, the solar irradiance changes quickly in a short period of time. The time profile comprises three irradiance levels. Solar exposition starts at 1000 W/m^2 and stays for 2 s. Then, it drops to 700 W/m^2 and lasts for 2 s. Again, it is reduced to 300 W/m^2. Figure 9a shows the maximum power tracking transient response of the four MPPT control variants plus the SGO–MPPT mechanism. Theoretical GMPPs, as a function of the solar radiation levels, were 798, 557.8 and 227.3 W, respectively. The measured solar energy harnessed by operating the MPPT control with SGO, DFO, ABC, PSOGS and PSO versions were 797.5, 797, 796, 795 and 794 W, respectively. Consequently, the harness efficiency numbers were 99.93%, 99.87%, 99.74%, 99.62% and 99.49%, respectively. Tracking performance in terms of settling time was also an important parameter. Therefore, the time recorded for SGO, DFO, ABC, PSOGS and PSO MPPTs to track maximum power was 0.22, 0.30, 0.38, 0.60 and 0.70 s, respectively. Figure 9b–d describes V_p, I_p and duty cycle d time evolution during the dynamic tracking process.

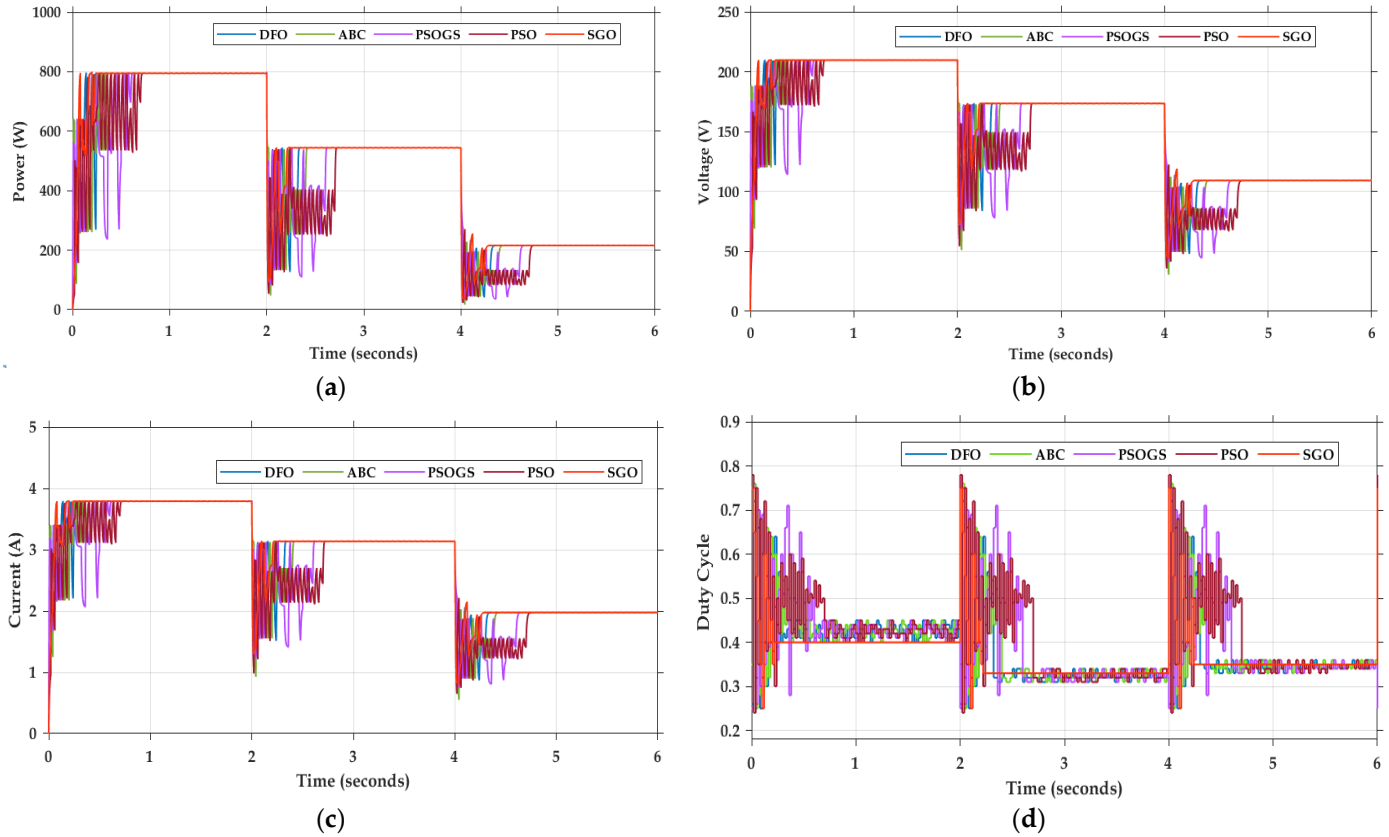

Figure 9. Case 1: comparison of (**a**) power, (**b**) voltage, (**c**) current, and (**d**) duty cycle of SGO, DFO, ABC, PSOGS, and PSO.

4.2.2. Case 2

Here, a non-uniform irradiation profile (500, 800, 1000 and 900 W/m^2) was generated for emulating a partial shading condition. Figure 10a–d shows the time information regarding the tracking process. From visual analysis, the PSO and PSOGS techniques

perform better in locating GMPP, yet the time to settle down was higher. Conversely, the DFO proved to be less efficient in tracking terms. The harnessed power in these operating conditions for SGO–MPPT was 503.5 W followed by DFO, ABC, PSO and PSOGS in descending order of GMPP (503.1, 502.1, 501 and 501.5 W). The settling times of SGO, DFO, ABC, PSOGS and PSO were 0.24, 0.46, 0.56, 0.62, and 0.87 s, respectively. Efficiencies achieved by SGO, DFO, ABC, PSO and PSOGS were 99.86%, 99.78%, 99.58%, 99.36%, and 99.46%, respectively.

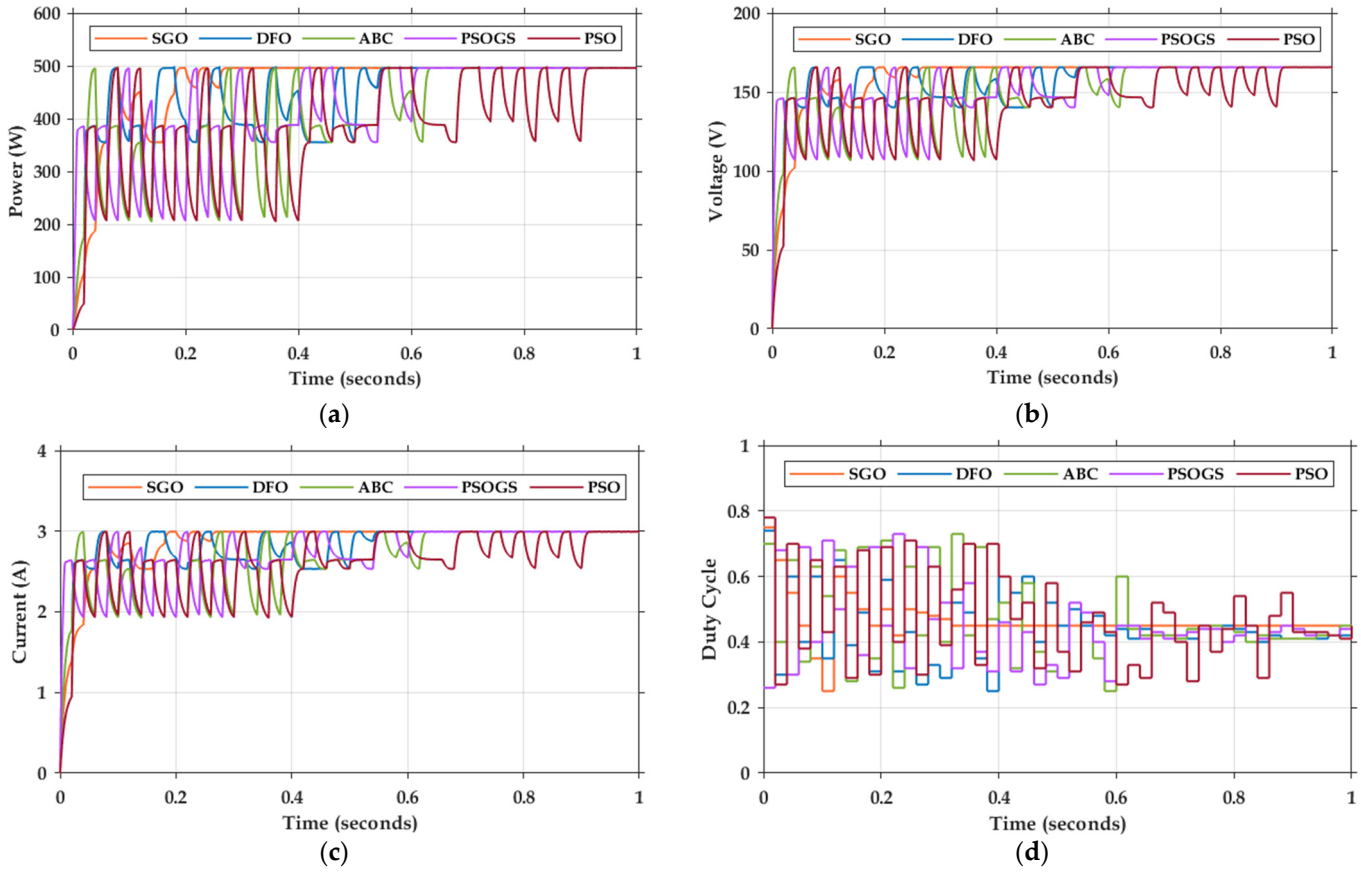

Figure 10. Case 2: comparison of (**a**) power, (**b**) voltage, (**c**) current, (**d**) duty cycle of SGO, DFO, ABC, PSOGS, and PSO.

4.2.3. Case 3

In the last scenario, the magnitude of the shading on each panel was increased, and the pattern was 800, 300, 700, and 550 W/m^2, respectively. The expected GMPP was 322.2W. The details concerning the mixed irradiance profile are available in Table 3. The maximum power tracking responses for the algorithms in comparison are shown in Figure 11. The power tracked by the SGO, DFO, ABC, PSO, and PSOGS were estimated as 321.5, 320.7, 320.1, 319.6, and 318.5 W, respectively, and their efficiencies were determined as 99.76%, 99.53%, 99.34%, 99.19%, and 98.85%, respectively. The convergence times of the SGO, DFO, ABC, PSOGS and PSO were 0.26, 0.50, 0.59, 0.69, and 0.89 s, respectively.

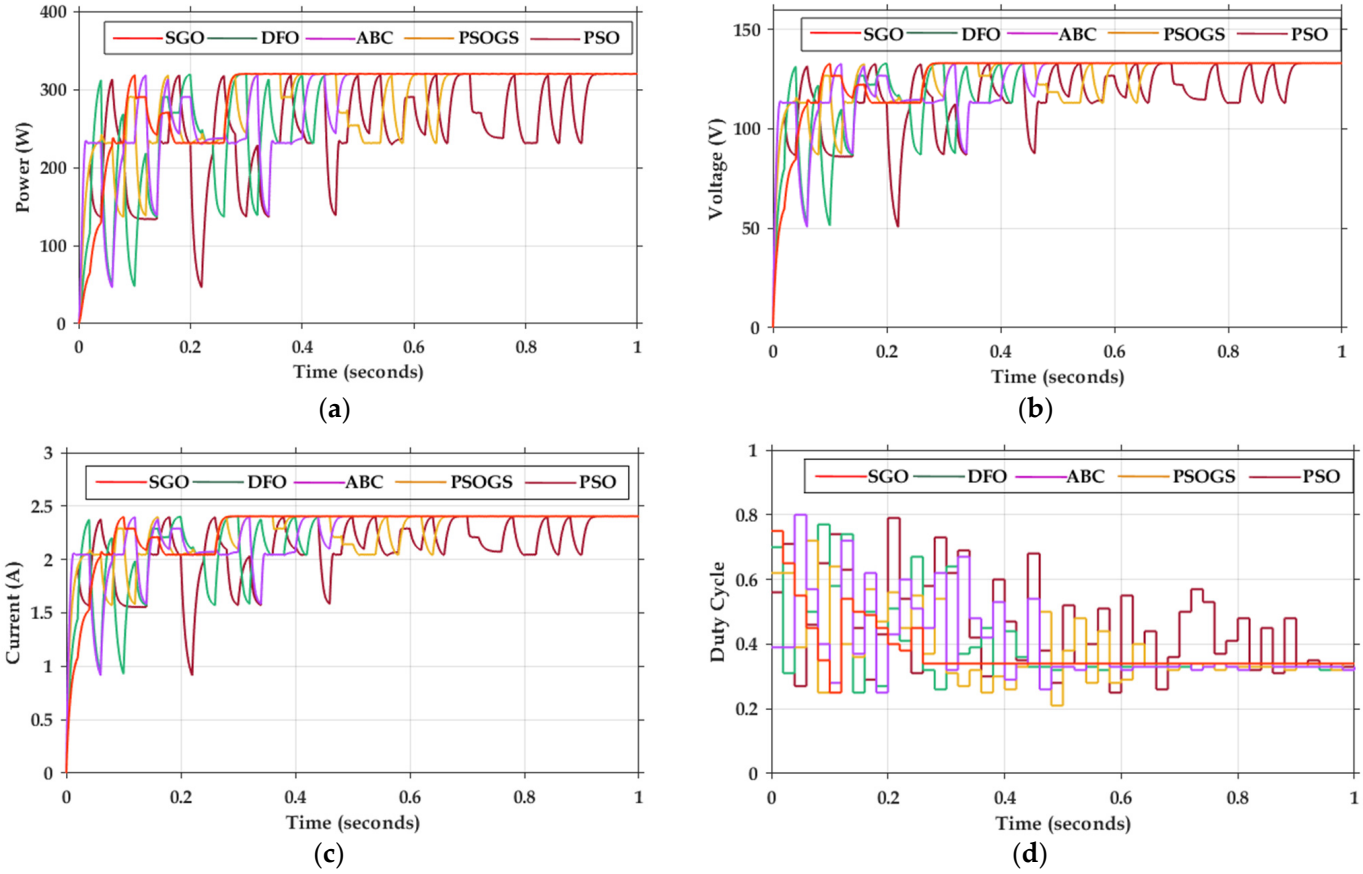

Figure 11. Case 3: comparison of (**a**) power, (**b**) voltage, (**c**) current, (**d**) duty cycle of SGO, DFO, ABC, PSOGS, and PSO.

4.3. Comparative Analysis

Statistical performance criteria were applied to evaluate SGO–MPPT vs. the other algorithm variants that were part of this study. Four statistical performance measurements were calculated [37], namely, *Efficiency (%)*, relative error (*RE*), mean absolute error (*MAE*) and root mean square error (*RMSE*), and they are defined by Equations (14)–(17).

$$Efficiency\ (\%) = \frac{PV_{tr}}{PV_p} \times 100 \tag{14}$$

$$RE = \frac{\sum_{i=1}^{h}(PV_p - PV_{tr,i})}{PV_{tr,i}} \times 100 \tag{15}$$

$$MAE = \frac{\sum_{i=1}^{h}(PV_p - PV_{tr,i})}{h} \tag{16}$$

$$RMSE = \sqrt{\frac{\sum_{i=1}^{h}(PV_p - PV_{tr,i})^2}{h}} \tag{17}$$

where PV_p is the measured global PV power, $PV_{tr,i}$ is the average power over the number of runs, which is calculated for each run I, and h is the total number of the runs.

Table 4 presents the statistical analysis results applied to the five MPPT algorithms. The comparison was carried out taking into account the three scenarios.

Table 4. Statistical analysis results.

Cases	Algorithms	Average Number of Iteration	GMPP (W)	Power Tracked (W)	Efficiency (%)	RE (%)	MAE	RMSE	Convergence Time (s)
Case 1	SGO	7.20	798 [1], 557.8 [2], 227.3 [3]	797.5, 557.3, 226.8	99.93	0.124	1.464	0.856	0.22
	DFO	10.28		797, 556.8, 226.3	99.87	0.249	2.929	1.711	0.3
	ABC	11.26		796, 555.8, 225.3	99.74	0.500	5.858	3.423	0.38
	PSOGS	12.19		795, 554.8, 224.3	99.62	0.752	8.787	5.134	0.6
	PSO	14.33		794, 553.8, 223.3	99.49	1.006	11.716	6.846	0.7
Case 2	SGO	10.68	504.2	503.5	99.86	0.139	2.050	1.198	0.24
	DFO	13.45		503.1	99.78	0.219	3.222	1.883	0.46
	ABC	14.26		502.1	99.58	0.418	6.151	3.594	0.56
	PSOGS	16.05		501.5	99.46	0.538	7.908	4.621	0.62
	PSO	18.34		501	99.36	0.639	9.373	5.477	0.87
Case 3	SGO	11.12	322.2	321.5	99.76	0.218	2.053	1.196	0.26
	DFO	14.90		320.7	99.53	0.468	4.393	2.567	0.5
	ABC	17.22		320.1	99.34	0.656	6.151	3.594	0.59
	PSOGS	21.62		319.6	99.19	0.814	7.615	4.450	0.69
	PSO	23.18		318.5	98.85	1.162	10.837	6.332	0.89

[1]: Global maximum power for 1000 W/m^2 irradiation; [2]: Global maximum power for 700 W/m^2; [3]: Global maximum power for 300 W/m^2.

The SGO convergence time was lower (0.20−0.26 s) compared to the other algorithms (0.30–0.80 s). In addition, the global maximum power value tracked by the SGO–MPPT was slightly higher when compared to other MPPT algorithms. Therefore, the efficiency acquired by the SGO–MPPT outplayed all the other state-of-the-art algorithms. For Case 2, the SGO algorithm achieved an efficiency of 99.86% with a convergence time of 0.24 s, despite the presence of partial shading conditions. However, the SGO in Case 3 produced better performance than the PSO. In all three cases, the average number of iterations of SGO for achieving global power peak was less than the other algorithms. The SGO–MPPT carried out here was a unidimensional search where the tracking was capable of finding the resultant power of the shaded multipower peaks. However, in a multidimensional search, the cumulative power of each shaded power peak would be added.

Each algorithm was independently run 10 times. It was observed that the RE, MAE, RMSE values of the PSO for Case 1 were 0.935, 10.642, and 6.218, respectively, which were much higher than that of the SGO (0.160, 1.856, 1.083). Similarly, error measures of the other algorithms and for the other cases were also higher than that of the SGO. Therefore, in terms of error measure, efficiency, average number of iterations and convergence time, SGO demonstrated the best performance.

5. Conclusions

This research work has presented an MPPT concept by adopting the SGO algorithm, which emulated individual human performance when they work as a team and prevailed in successfully tracking the global power peak among the other local peaks in a shaded PV array. The suggested SGO not only prevailed in grasping the global power peak but also outperformed the capabilities of the other well-entrenched global search algorithms such as DFO, ABC, PSOGS, and PSO, in terms of convergence time and efficiency. The versality of the SGO–MPPT over the other counterparts was proven when all these algorithms were subjected to an attempt to grasp the peak power under three challenging conditions, such as abrupt variations in irradiance and nonlinear shading patterns. The convergence time of SGO–MPPT has a clear edge over other global search counterparts, and notably, it was 26% and 47% ahead with its closest counterparts DFO and ABC, respectively. The peak power tracked was always more than that of all the other compared MPPT schemes. In addition, the SGO–MPPT can be extended for a multidimensional search-distributed MPPT scheme, which can further increase the net power output.

Author Contributions: All authors had equal contribution to prepare and finalise the manuscript. Conceptualisation, S.V., B.C.S. and S.R., methodology, S.V., B.C.S., S.R., M.A., J.H. and E.M.G.R.; software, S.V., B.C.S. and S.R.; validation, S.V., B.C.S., S.R., M.A., J.H. and E.M.G.R.; formal analysis, S.V., B.C.S., S.R., M.A., J.H. and E.M.G.R.; investigation, S.V., B.C.S. and S.R.; resources, B.C.S. and S.R.; data curation, S.V., B.C.S. and S.R.; writing—original draft preparation, S.V., B.C.S. and S.R.; writing—review and editing, S.V., B.C.S., S.R., M.A., J.H. and E.M.G.R.; visualization, B.C.S., S.R., M.A., J.H. and E.M.G.R.; supervision, B.C.S., S.R., M.A., J.H. and E.M.G.R.; project administration, B.C.S. and S.R. All authors have read and agreed to the published version of the manuscript.

Funding: This research received no external funding.

Institutional Review Board Statement: Not applicable.

Informed Consent Statement: Not applicable.

Data Availability Statement: The data presented in this study are available in article.

Acknowledgments: The authors would such as to thank the team at Manchester Met. University and University of York for supporting this research work and preparing the manuscript.

Conflicts of Interest: The authors declare no conflict of interest.

Nomenclature

PV	Photovoltaic
MPPT	Maximum Power Point Tracking
PS	Partial Shading
SGO	Social Group Optimization
PSO	Particle Swarm Optimization
DFO	Dragon Fly Algorithm
ABC	Artificial Bee Colony Algorithm
Vmp	Peak Operating Voltage
P&O	Perturb and Observe
INC	Incremental Conductance
S	Separation
c	Cohesion
e	Position of the Enemy
w	Inertia Weight
OCV	Open Circuit Voltage
SCC	Short Circuit Current
GA	Genetic Algorithm
PSOGS	Particle Swarm Optimization Gravitation Search
ANN	Artificial Neural Network
DE	Differential Evolution
ACO	Ant Colony Algorithm
GWO	Grey Wolf Optimizer
STC	Standard Test Conditions
GMPP	Global Maximum Power Point
a	Alignment
f	Position of the Food
C1, C2	Cognitive Factor
GO	Regulatory Co-efficient

References

1. Shaw, S.; Libby, C.; Scott, M.; Grice, L.N.; Shaikh, N.; Peterson, C.; Ladwig, K. The Global Circular Economy for the Electric Power Industry and Opportunities for Solar Photovoltaics. In Proceedings of the 2021 IEEE 48th Photovoltaic Specialists Conference (PVSC), Fort Lauderdale, FL, USA, 20–25 June 2021. [CrossRef]
2. Renewables 2020. Available online: https://www.iea.org/reports/renewables-2020 (accessed on 1 March 2022).
3. Kumar, J.C.R.; Majid, M.A. Renewable energy for sustainable development in India: Current status, future prospects, challenges, employment, and investment opportunities. *Energy Sustain. Soc.* **2020**, *10*, 1–36. [CrossRef]

4. D'Adamo, I.; Gastaldi, M.; Morone, P. The post COVID-19 green recovery in practice: Assessing the profitability of a policy proposal on residential photovoltaic plants. *Energy Policy* **2020**, *147*, 111910. [CrossRef]
5. Dhimish, M.; Holmes, V.; Mather, P.; Sibley, M. Novel hot spot mitigation technique to enhance photovoltaic solar panels output power performance. *Sol. Energy Mater. Sol. Cells* **2018**, *179*, 72–79. [CrossRef]
6. Bollipo, R.B.; Mikkili, S.; Bonthagorla, P.K. Hybrid, optimal, intelligent and classical PV MPPT techniques: A review. *CSEE J. Power Energy Syst.* **2020**, *19*, 9–33.
7. Ahmad, R.; Murtaza, A.F.; Sher, H.A. Power tracking techniques for efficient operation of photovoltaic array in solar applications—A review. *Renew. Sustain. Energy Rev.* **2019**, *101*, 82–102. [CrossRef]
8. FerozMirza, A.; Mansoor, M.; Ling, Q.; Khan, M.I.; Aldossary, O.M. Advanced Variable Step Size Incremental Conductance MPPT for a Standalone PV System Utilizing a GA-Tuned PID Controller. *Energies* **2020**, *13*, 4153. [CrossRef]
9. Shahid, H.; Kamran, M.; Mehmood, Z.; Saleem, M.Y.; Mudassar, M.; Haider, K. Implementation of the novel temperature controller and incremental conductance MPPT algorithm for indoor photovoltaic system. *Sol. Energy* **2018**, *163*, 235–242. [CrossRef]
10. Ammar, H.H.; Azar, A.T.; Shalaby, R.; Mahmoud, M.I. Metaheuristic optimization of fractional order incremental conductance (FO-INC) maximum power point tracking (MPPT). *Complexity* **2019**, *2019*, 7687891. [CrossRef]
11. Paul, S.; Thomas, J. Comparison of MPPT using GA optimized ANN employing PI controller for solar PV system with MPPT using incremental conductance. In Proceedings of the 2014 International Conference on Power Signals Control and Computations (EPSCICON), Thrissur, India, 6–11 January 2014. [CrossRef]
12. Ibrahim, A.W.; Shafik, M.B.; Ding, M.; Sarhan, M.A.; Fang, Z.; Alareqi, A.G.; Almoqri, T.; Al-Rassas, A.M. PV maximum power-point tracking using modified particle swarm optimization under partial shading conditions. *Chin. J. Electr. Eng.* **2020**, *6*, 106–121. [CrossRef]
13. Mirza, A.F.; Ling, Q.; Javed, M.Y.; Mansoor, M. Novel MPPT techniques for photovoltaic systems under uniform irradiance and Partial shading. *Sol. Energy* **2019**, *184*, 628–648. [CrossRef]
14. Eltamaly, A.M.; Farh, H.M.H. Dynamic global maximum power point tracking of the PV systems under variant partial shading using hybrid GWO-FLC. *Sol. Energy* **2019**, *177*, 306–316. [CrossRef]
15. Ulaganathan, M.S.; Devaraj, D. A novel MPPT controller using Neural Network and Gain-Scheduled PI for Solar PV system under rapidly varying environmental condition. *J. Intell. Fuzzy Syst.* **2019**, *37*, 1085–1098. [CrossRef]
16. Lin, W.; Lian, Z.; Gu, X.; Jiao, B. A Local and Global Search Combined Particle Swarm Optimization Algorithm and Its Convergence Analysis. *Math. Probl. Eng.* **2014**, *2014*, 905712. [CrossRef]
17. Figueiredo, S.; e Silva, R.N.A.L. Hybrid MPPT Technique PSO-P&O Applied to Photovoltaic Systems Under Uniform and Partial Shading Conditions. *IEEE Lat. Am. Trans.* **2021**, *19*, 1610–1617. [CrossRef]
18. Tavakoli, A.; Forouzanfar, M. A self-constructing Lyapunov neural network controller to track global maximum power point in PV systems. *Int. Trans. Electr. Energy Syst.* **2020**, *30*, 12391. [CrossRef]
19. Tey, K.S.; Mekhilef, S.; Yang, H.-T.; Chuang, M.-K. A Differential Evolution Based MPPT Method for Photovoltaic Modules under Partial Shading Conditions. *Int. J. Photoenergy* **2014**, *2014*, 945906. [CrossRef]
20. Priyadarshi, N.; Ramachandaramurthy, V.K.; Padmanaban, S.; Azam, F. An ant colony optimized MPPT for standalone hybrid PV-wind power system with single Cuk converter. *Energies* **2019**, *12*, 167. [CrossRef]
21. Soufyane Benyoucef, A.; Chouder, A.; Kara, K.; Silvestre, S. Artificial bee colony based algorithm for maximum power point tracking (MPPT) for PV systems operating under partial shaded conditions. *Appl. Soft Comput.* **2015**, *32*, 38–48. [CrossRef]
22. Darcy GnanaJegha, A.; Subathra, M.S.P.; Manoj Kumar, N.; Subramaniam, U.; Padmanaban, S. A High Gain DC-DC Converter with Grey Wolf Optimizer Based MPPT Algorithm for PV Fed BLDC Motor Drive. *Appl. Sci.* **2020**, *10*, 2797. [CrossRef]
23. Zhang, Y.; Jin, Z. Group teaching optimization algorithm: A novel metaheuristic method for solving global optimization problems. *Expert Syst. Appl.* **2020**, *148*, 113246. [CrossRef]
24. Motahhir, S.; El Hammoumi, A.; El Ghzizal, A. The most used MPPT algorithms: Review and the suitable low-cost embedded board for each algorithm. *J. Clean. Prod.* **2020**, *246*, 118983. [CrossRef]
25. Rezk, H.; Fathy, A.; Abdelaziz, A.Y. A comparison of different global MPPT techniques based on meta-heuristic algorithms for photovoltaic system subjected to partial shading conditions. *Renew. Sustain. Energy Rev.* **2017**, *74*, 377–386. [CrossRef]
26. Zafar, M.H.; Al-shahrani, T.; Khan, N.M.; Feroz Mirza, A.; Mansoor, M.; Qadir, M.U.; Naqvi, R.A. Group Teaching Optimization Algorithm Based MPPT Control of PV Systems under Partial Shading and Complex Partial Shading. *Electronics* **2020**, *9*, 1962. [CrossRef]
27. Satapathy, S.; Naik, A. Social group optimization (SGO): A new population evolutionary optimization technique. *Complex Intell. Syst.* **2016**, *2*, 173–203. [CrossRef]
28. Cherukuri, S.K.; Balachandran, P.K.; Kaniganti, K.R.; Buddi, M.K.; Butti, D.; Devakirubakaran, S.; Alhelou, H.H. Power Enhancement in Partial Shaded Photovoltaic System Using Spiral Pattern Array Configuration Scheme. *IEEE Access* **2021**, *9*, 123103–123116. [CrossRef]
29. Palpandian, M.; Winston, D.P.; Kumar, B.P.; Kumar, C.S.; Babu, T.S.; Alhelou, H.H. A New Ken-Ken Puzzle Pattern Based Reconfiguration Technique for Maximum Power Extraction in Partial Shaded Solar PV Array. *IEEE Access* **2021**, *9*, 65824–65837. [CrossRef]
30. Winston, P.; Kumar, B.P.; Christabel, S.C.; Chamkha, A.J.; Sathyamurthy, R. Maximum Power Extraction in Solar Renewable Power System—A Bypass Diode Scanning Approach. *Comput. Electr. Eng.* **2018**, *70*, 122–136. [CrossRef]

31. Mansoor, M.; Mirza, A.F.; Ling, Q.; Javed, M.Y. Novel Grass Hopper optimization based MPPT of PV systems for complex partial shading conditions. *Sol. Energy* **2020**, *198*, 499–518. [CrossRef]
32. Sundaram, B.M.; Manikandan, B.V.; Kumar, B.P.; Winston, D.P. Combination of Novel Converter Topology and Improved MPPT Algorithm for Harnessing Maximum Power from Grid Connected Solar PV Systems. *J. Electr. Eng. Technol.* **2019**, *14*, 733–746. [CrossRef]
33. Singh, G.K.; Kaur, A. Maximum Power Point Tracking in Photovoltaic Solar Energy Systems using Hybrid PSO-GSA Method. *Int. J. Eng. Res. Technol.* **2015**, *4*, 391–394.
34. Raman, G.; Raman, G.; Manickam, C.; Ganesan, S.I. Dragonfly Algorithm Based Global Maximum Power Point Tracker for Photovoltaic Systems. *Lect. Notes Comput. Sci.* **2016**, *9712*, 211–219. [CrossRef]
35. Shams, I.; Mekhilef, S.; Tey, K.S. Maximum Power Point Tracking Using Modified Butterfly Optimization Algorithm for Partial Shading, Uniform Shading, and Fast Varying Load Conditions. *IEEE Trans. Power Electron.* **2021**, *36*, 5569–5581. [CrossRef]
36. Parvaneh, M.H.; Khorasani, P.G. A new hybrid method based on fuzzy logic for maximum power point tracking of photovoltaic systems. *Energy Rep.* **2020**, *6*, 1619–1632. [CrossRef]
37. Yousri, D.; Babu, T.S.; Allam, D.; Ramachandaramurthy, V.K.; Etiba, M.B. A Novel Chaotic Flower Pollination Algorithm for Global Maximum Power Point Tracking for Photovoltaic System under Partial Shading Conditions. *IEEE Access* **2019**, *7*, 121432–121445. [CrossRef]